

Surface Hardness Modification of Selective Laser Melted Ti6Al4V Parts by Sliding Friction Diamond Burnishing

Gergely Dezső^{1*}, Ferenc Szigeti¹, Gyula Varga²

¹ Department of Physics and Production Engineering, Institute of Engineering and Agricultural Science, University of Nyíregyháza, Sóstói út 31/B, H-4400 Nyíregyháza, Hungary

² Institute of Manufacturing Science, Faculty of Mechanical Engineering and Informatics, University of Miskolc, Egyetemváros 1., H-3515 Miskolc, Hungary

* Corresponding author, e-mail: dezso.gergely@nye.hu

Received: 03 September 2022, Accepted: 06 November 2022, Published online: 22 November 2022

Abstract

Selective laser melting (SLM) is a frequently used additive manufacturing technology for creating metallic, especially Ti6Al4V parts. After the production by SLM usually postprocessing is necessary for several reasons. Here the sliding friction diamond burnishing is applied as postprocessing procedure.

In this paper an experimental study of surface hardness improvement of selective laser melted Ti6Al4V ELI cylindrical parts is demonstrated. The surface is modified by sliding friction diamond burnishing as postprocessing machining. The design of experiment method was applied to investigate effect of five factors (two SLM and three machining parameters) on surface hardness modification. It is shown that both SLM and postprocessing factors makes significant effect to the surface hardness improvement, most important ones are laser power, laser scan speed during manufacturing, and the burnishing force as factor of postprocessing. Empirical formulas are fit to measurement data, and visualized by surface plots. Relationship between factors and the surface hardness improvement is strongly nonlinear. In the investigated parameter window burnishing force has always positive effect to surface hardness improvement. Electron microscopic investigations show that change in surface hardness can be related to four main morphological changes: compression of the surface by plastic deformation of protrusions, attenuation of valleys, formation of inner cavities and creation of small protrusions by diamond tool. This paper is an extended paper of a conference paper published in the proceedings book of the XXXI. International Welding Conference (Kecskemét, Hungary).

Keywords

selective laser melting, surface hardness, diamond burnishing, Ti6Al4V, additive manufacturing

1 Introduction

Additive manufacturing (AM) is an expansive division of production technologies which enables us to manufacture parts with almost arbitrary geometries on the same machine directly from the CAD body model. Most frequently applied one of seven class of additive manufacturing is family of powder bed fusion (PBF) technologies [1]. Direct metal selective laser melting (DMSLM, or here referred as SLM) today widely applied for manufacturing metallic parts [2, 3]. This technology creates parts from a special metal powder layer by layer using laser beam for melting it within inert gas atmosphere.

However completely ready for use products can be made only in a few case depending on application and certain type of AM technology.

Postprocessing today is an integral part of production by additive manufacturing technologies [4]. Main reasons why postprocessing is necessary are dimensional and shape accuracy, surface quality [5–8], classical machining [9] such details which need special accuracy of possibly can be made much more cost effectively in this way. Surface treatment may significantly affect also fracture and fatigue properties [10].

Nowadays burnishing processes are widely studied as methods for surface modification, especially for improving wear resistance, surface hardness and surface roughness [11]. Good results were published in surface hardness and fatigue improvement for steel alloys (AISI 316Ti) [12], surface roughness, residual stress, and wear resistance

doing-up of a hardened steel [13] effect to surface roughness and hardness in case of carbon steel [14].

Effects of burnishing procedure to titanium alloys has been investigated in two cases accordingly the test specimens are wrought or additively manufactured.

Burnishing studies of wrought titanium alloys showed that beyond machining parameters also lubricants may have significant effect to surface hardness, wear resistance and fatigue [15, 16], roller burnishing experiments of Ti4Al4V show that significant improvement of surface roughness and hardness can be achieved even in cryogenic conditions [17].

In case of additively manufactured metallic parts burnishing has been conceived as a postprocessing procedure [18, 19]. Burnishing experiments of additively manufactured steel [20, 21], aluminum [22], nickel [23] alloys are published. We have found a research gap in the topic of surface hardness modification by sliding friction diamond burnishing of additively manufactured Ti6Al4V parts. This is the motivation of recent study.

2 Materials and methods

In Section 2 four important topics are detailed:

1. Material of samples, Ti6Al4V is widely used and studied, but it was not investigated in case of it was produced by SLM and postprocessed by sliding friction diamond burnishing.
2. Inward and surface structure of specimens are determined by the production method, SLM. Parameters of SLM may also influence machinability of the surface.
3. Sliding friction diamond burnishing is introduced. Here we study its effect to surface hardness.
4. Experimental methods namely hardness test and electron microscopic methods are also described.

2.1 Material

Ti6Al4V is a titanium alloy widely used in medical, pharmaceutical, food, aeronautical and marine vehicle, nuclear industries, and many other fields [24]. It is applied in wrought and additively manufactured form [25, 26]. Main advantages of this material are high mass-strength ratio, chemical endurance, and biocompatibility. Disadvantage of this alloy is that it has poor tribological properties, namely weak wear resistance and unstable friction coefficient [27].

We applied Ti6Al4V with extra low interstitials (ELI), which a pure version of this alloy with enhanced ductility

and strength. Chemical composition of Ti6Al4V can be contained Table 1 [28].

2.2 Selective laser melting

Selective laser melting (SLM) is an additive manufacturing (AM) technology. It belongs to class of powder bed fusion (PBF) of seven classes of AM technologies. Fusion can be achieved in several ways, for example sintering (without melting of the material), melting by electron beam or laser beam. In our experiments we applied a machine which melts the material by a laser beam.

SLM is mainly used for plastics and metals. For metals laser power is higher than for plastics.

When SLM is applied for metals, it is often called direct metal selective laser melting (DMSLM), but here we will refer to this procedure simply as SLM, because we used only one material and only one technology, so it is impossible to misunderstand.

Feedstock of SLM is powder. Chemical composition of this powder is identical to the material produced by SLM. Average size, size distribution and shape of powder particles depends on the process of powder production. Data regarding it is determined experimentally and provided by the manufacturer. In our experiments size of powder particles changed from 20 to 80 micrometers.

Mechanism of SLM is layer by layer building. A blade spreads precisely a layer of metal powder. Layer thickness is an important parameter of SLM, it can be varied, but we kept it constant. In our work layer thickness was always 0.03 mm. Then the laser beam scans the layer of the powder according to the geometry of the part to be manufactured. Infill laser power (P) and infill laser scanning speed (u) are also important processing parameters and in our work those were varied. We go into details later regarding processing parameters. We mention that hatch distance was constant 0.14 mm in our experiments.

During SLM procedure powder is in a chamber filled with inert gas, in our case it was argon (Ar).

Our specimens were produced by an EOS M290 400W machine.

Table 1 Chemical Composition of Ti6Al4V ELI All values are in weight %; *Other1: maximum each of other elements; **Other2: maximum total of other elements

C	O	N	H	Fe
≤0.08	≤0.20	≤0.05	≤0.015	≤0.40
Al	V	*Other1	**Other2	Ti
5.5~6.75	3.5~4.5	≤0.1	≤0.4	rest

It must be noted that SLM procedure has several processing parameters what can be varied. We used default values of all parameters excepted above mentioned two: P and u which were handled as factors of experiments.

2.3 Sliding friction diamond burnishing

Sliding friction burnishing is kinematically similar to turning, but instead of the edge of the single point cutting tool, the burnishing tool having spherical end pressed to the surface to be machined. The method creates a plastic deformation on the surface of the machined workpiece and in the near-surface layers (Fig. 1) [29].

Sliding friction burnishing tools can be used on all conventional and CNC controlled lathes or CNC turning centers. Thus, immediately after machining, the workpieces can be burnished in the same clamping as the machining. Sliding friction burnishing can be used to treat outer cylindrical surfaces, large diameter inner cylindrical surfaces, but even flat surfaces as well. The main technical and technological parameters of the production of the sliding friction burnishing process: the radius of the spherical end tip of the deforming element r , mm; burnishing force F (or F_b) (N); feed f (mm/rev); burnishing speed v (m/min). Additional factors include the number of burnishing passes i and the type of lubricant. The technology of reinforcement has been studied by several people on different material qualities, with different tools, in order to meet different expected requirements. Examples, without wishing to be exhaustive, are as follows.

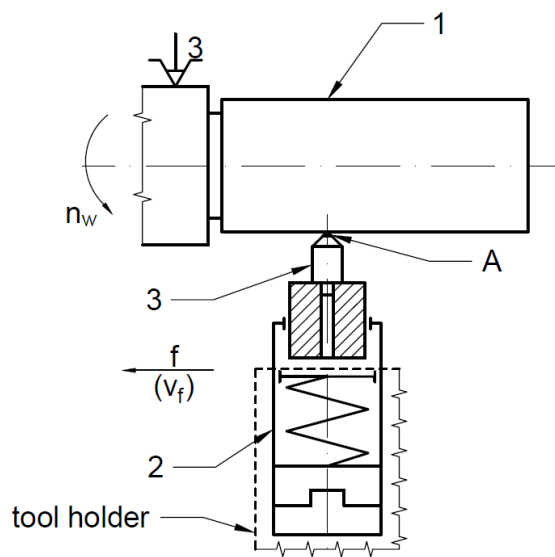


Fig. 1 A schematic diagram of sliding friction burnishing (1—workpiece, 2—burnishing tool, 3—burnishing insert, A—active element of tip) (adapted from [8])

Total surface integrity was analyzed by Rotella et al. [30] in terms of surface roughness, microhardness, microstructural changes, and tribology. In particular, the results obtained showed that cryogenic cooling conditions and coating significantly improve the hardness of the burnished workpiece, while MQL lubrication leads to excellent surface roughness.

A study by Samatham et al. [31] deals with the study of different burnishing processes in the titanium alloy Ti6Al4V. According to their study, cryogenic burnishing is one of the latest innovation techniques using liquid nitrogen for cooling.

In their study, Toboła et al. [32] subjected the Ti6Al4V alloy to a multi-step hybrid treatment, including turning and burnishing and gas nitriding. They found that the use of sliding friction burnishing and low temperature gas nitriding increases the surface hardness by 5–10% without compromising the strength of the substrate material.

2.4 Experimental methods

The surface of the selective laser sintered specimens was uneven and unsuitable for hardness measurement, therefore, in preparation, a smooth turning was performed on the circumferential surface of the specimens with a 0.25 mm depth of cut, which reduced the diameter of the specimens to 9.5 mm. The surface hardness measurement was executed on a hardness measuring machine type HPO-250, with a test load of $F_h = 98.07$ N, performed at 3 locations on the mantle surface of the specimens at 120° , and then the mean and standard deviation of the measurements were determined (Fig. 2).

The hardness values HV10 Vickers were determined according to the standard MSZ EN ISO 6507-1: 2018 [33],

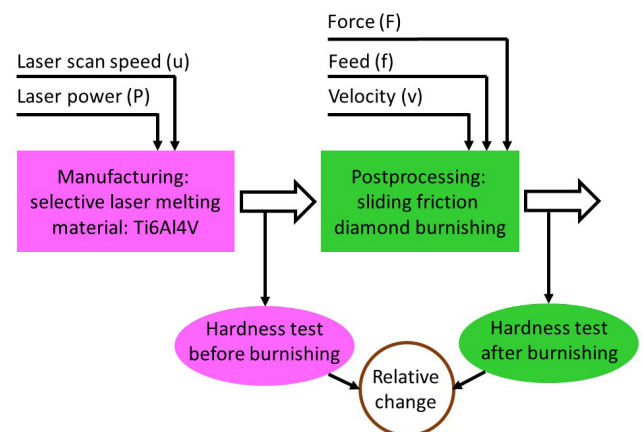


Fig. 2 Overall scheme and factors of experimental work

using a 136° diamond pyramid test specimen based on Eq. (1):

$$HV = 0.102 \cdot \frac{2F_h \cdot \sin \frac{136^\circ}{2}}{d^2} = 0.1891 \frac{F_h}{d^2}, \quad (1)$$

where:

- d : average of the indentation values,
- F_h : test load ($F_h = 98.07$ N for HV10).

When measuring the surface hardness, the hardness determined on cylindrical surfaces according to MSZ EN ISO 6507-1: 2018 shall be calculated. Therefore, the HV10 value determined from the indentation diagonals measured on the cylindrical surface was multiplied for each measurement by the correction factor shown in [33]. The tables of HV10 measurement results reported on cylindrical surfaces in Section 3 contain the HV10 hardness values calculated by Eq. (1).

Electron microscopic images were captured by a HITACHI SU1510 scanning electron microscope to observe morphological changes on cylinder side caused by sliding friction burnishing. We investigated it on the edge of polished cross sections.

3 Design of experiment and sample production

Samples were solid cylinders 50 mm in length and 10 mm in diameter.

Before going into details one must see the overall scheme of our experiments. We selected five factors, two of those influenced SLM procedure, and three of those were machining parameters. Fig. 2 shows main steps of experimental work, and factors belonging to each step. Surface hardness was measured before burnishing (that is after manufacturing) on the raw surface, and after burnishing. Objective of our experimental work was to establish relative change of surface hardness resulted by diamond burnishing.

Cylindrical test samples were produced for experiments by selective laser melting. Five groups of specimens were prepared according to Table 2. Specimens in a group produced by the same SLM technology parameters, but different groups had different parameters. Groups are denoted by letters A, B, C, D, E. There were 8 specimens in each group.

Two manufacturing parameters varied between groups: infill laser power and infill laser scan speed. Values are presented in Table 2. All other selective laser melting parameters kept constant. Table 3 shows two important

Table 2 Additive manufacturing parameters of producing the specimens

Code of parameter setup	Infill laser power (W)	Infill laser scan speed (mm/s)
A	233.33	1200
B	280.00	1000
C	336.00	1441
D	233.33	1000
E	280.00	1200

Table 3 Burnishing parameters

No	Speed v (m/min)	Feed f (mm/rev)	Force F (N)
1	8.321	0.0125	80
2	11.775	0.0125	80
3	8.321	0.0500	80
4	11.775	0.0500	80
5	8.321	0.0125	120
6	11.775	0.0125	120
7	8.321	0.0500	120
8	11.775	0.0500	120

parameters, layer thickness and hatch distance which also were the same for each specimen, their values was equal to default values of the machine: hatch distance (h) 0.14 mm, laser type: Yb fiber laser with wavelength 1060–1100 nm, focus diameter 100 μ m, no pattern option for exposure strategy, exposure mode: single. Layer thickness (t) was set to 0.03 mm, and kept constant for each specimen.

Parameter set E ($P = 280$ W, $u = 120$ mm/s) comes from the default setting of the EOS M290 400W SLM machine. Other SLM parameter settings may be compared by so-called energy input, which is specific power flow density referring to volume unit (1 mm³), it is denoted by e , calculated by the formula $e = P/uh$. For sets C, D and E energy input is the same, namely 55.5 W/mm³. For A it is 46.3 W/mm³, for B 66.7 W/mm³.

The burnishing procedure was performed by a natural PCD tool having a radius of $R = 3.5$ mm. In the experiments executed, three factors were applied: burnishing speed (v), feed (f) and burnishing force (F). In case three factors, by using the full factorial experiment design method the number of the experiments are $n = 8$, because all the factors are set to a minimum and a maximum value. These combinations can be seen in Table 3. In determining the numerical values, we took into account the results of our previous theoretical and practical research.

These technological parameters were used for all the additively manufactured specimen. Logic of notations of

specimens: for specimens produced by additive manufacturing parameters belonging to "A" (Table 2) burnished by technological parameters "1" (Table 3) denoted A1 (can be found in Table 4).

Table 4 Measured HV10 values and calculated improvement ratios

Code	HV10 Before burnishing	HV10 After burnishing	IRHV %
A1	365	406	11.04
A2	377	357	-5.24
A3	362	398	9.98
A4	387	357	-7.64
A5	373	432	15.90
A6	368	393	6.77
A7	366	394	7.79
A8	378	392	3.74
B1	387	394	1.79
B2	374	365	-2.24
B3	370	392	5.93
B4	383	396	3.47
B5	375	388	2.12
B6	359	426	18.73
B7	373	357	-4.54
B8	366	383	4.61
C1	399	392	-1.80
C2	388	385	-0.92
C3	379	394	4.07
C4	397	387	-2.54
C5	382	369	-3.33
C6	376	404	7.38
C7	357	383	7.28
C8	383	384	0.50
D1	381	373	-2.21
D2	378	367	-2.92
D3	376	356	-5.39
D4	391	369	-5.68
D5	379	338	-10.92
D6	380	408	7.21
D7	384	371	-3.59
D8	374	370	-1.17
E1	389	395	1.83
E2	384	358	-6.81
E3	374	344	-8.00
E4	376	365	-3.17
E5	380	367	-3.33
E6	381	351	-7.87
E7	396	391	-1.10
E8	368	415	12.49

4 Results

For evaluation of measured hardness value improvements by burnishing, improvement ratios were introduced, which are shown in Eq. (2) [15]:

$$IRHV = \frac{HV_a - HV_b}{HV_b} \cdot 100\%, \quad (2)$$

where:

- IRHV – the ratio of surface hardness improvement (%),
- HV_a – the surface hardness after burnishing process,
- HV_b – the surface hardness before burnishing process.

The average of the measured data and the calculated improvement ratios are summarized in Table 4.

Fig. 3 shows test specimens before and after postprocessing. The top half of the cylinders on Fig. 3 has the original raw surface. Bottom part of Fig. 3 shows postprocessed, that is burnished surface.

5 Evaluation of results

Since we have five factors, we calculated main effects and interactions. Factor effects and interactions were calculated from IRHV data of sample sets A, B, D and E, since those form a 5-factor and 2-level full factorial experiment with 8 items in each set. Table 5 shows main effect values for all factors, Table 6 demonstrates interactions.

In Table 5 largest value of main effects belongs to force, and it has positive sign. It implies that burnishing force has significant impact to surface hardness improvement. However other four main effects are not negligible related to main effect of burnishing force. Second largest main effect belongs to laser power P , which is a manufacturing



Fig. 3 Samples before and after postprocessing: The upper part of the picture shows raw surface, and bottom part the burnished surface

Table 5 Main effects of factors to IRHV (surface hardness improvement ratio): Factors P and u are SLM processing parameters (purple), v, f and F are postprocessing machining parameters (green)

P	-5.97
u	-2.85
v	-1.26
f	-3.07
F	7.35

Table 6 Interactions of experimental factors on IRHV (surface hardness improvement ratio) value: Factors P and u are SLM processing parameters, v, f and F are postprocessing machining parameters

Pu	-10.78	uv	-5.62	vf	-5.30
Pv	10.97	uf	-2.33	vF	10.53
Pf	-1.41	uF	1.10	fF	-4.24
PF	-2.42				

parameter. This indicates that surface hardness improvement is influenced by all factors, namely by both manufacturing, that is SLM processing parameters (P, u) and post-processing, that is burnishing parameters (v, f, F).

There can be seen three interaction term with relatively large value in Table 6. Large interaction term of P and u points to that SLM manufacturing parameters make effect to surface hardness improvement under postprocessing, that is machinability. Second term of P and v connects a production factor with a postprocessing factor. Third interaction term concerns two postprocessing factor v and F . By these values one can strengthen the proposition that surface hardness improvement is determined by all five factors also with interactions between those.

Empirical functions were fitted to measurement data for each sample set (A, B, C, D, E), and for two different force (F) value. Variables of these functions are feed (f) and machining velocity (v). Software MATHCAD 15.0 was applied for function fitting. Algebraic formulas of empirical functions are shown in Eqs. (3)–(7), and Figs. 4–8 visualize surfaces defined by those. Each figure demonstrates empirical functions fitted to data of a given group of samples denoted by A–D, and shows two surfaces belonging the two different values of burnishing force (F).

$$IRHV_A = 59.2715 - 7.488v + 1260f - 0.122F - 109.523vf + 0.036vF - 15.017fF + 1.239vfF \quad (3)$$

$$IRHV_B = 117.5395 - 15.02v - 574.914f - 1.327F + 151.578vf + 0.171vF + 7.301fF - 1.743vfF \quad (4)$$

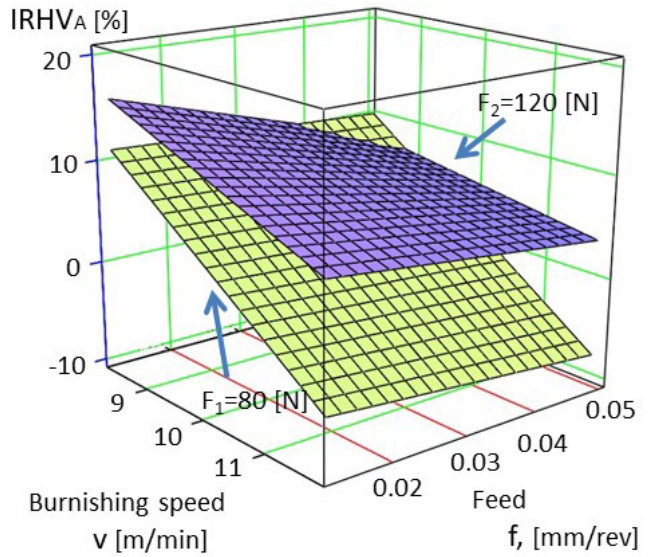


Fig. 4 Surface hardness improvement ratio (IRHV) for sample set A, as function of burnishing speed (v), and feed (f), according to experimental formula Eq. (3)

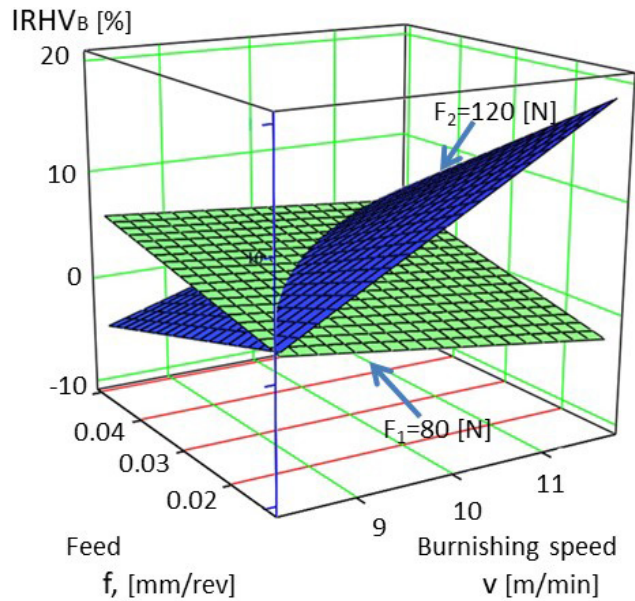


Fig. 5 Surface hardness improvement ratio (IRHV) for sample set B, as function of burnishing speed (v), and feed (f), according to experimental formula Eq. (4)

$$IRHV_C = 57.6222 - 6.632v - 896.336f - 0.869F + 96.238vf + 0.095vF + 19.189fF - 1.927vfF \quad (5)$$

$$IRHV_D = 142.1163 - 14.279v - 2.747 \cdot 10^3 f - 1.765F + 252.534vf + 0.175vF + 32.933fF - 3.115vfF \quad (6)$$

$$IRHV_E = 67.4341 - 5.283v - 1172f - 0.38F + 252.534vf + 0.175vF + 32.933fF - 3.115vfF \quad (7)$$

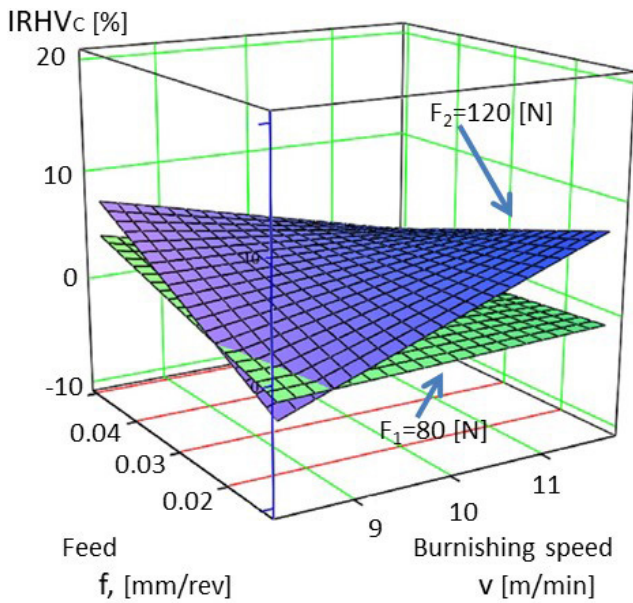


Fig. 6 Surface hardness improvement ratio (IRHV) for sample set C, as function of burnishing speed (v), and feed (f), according to experimental formula Eq. (5)

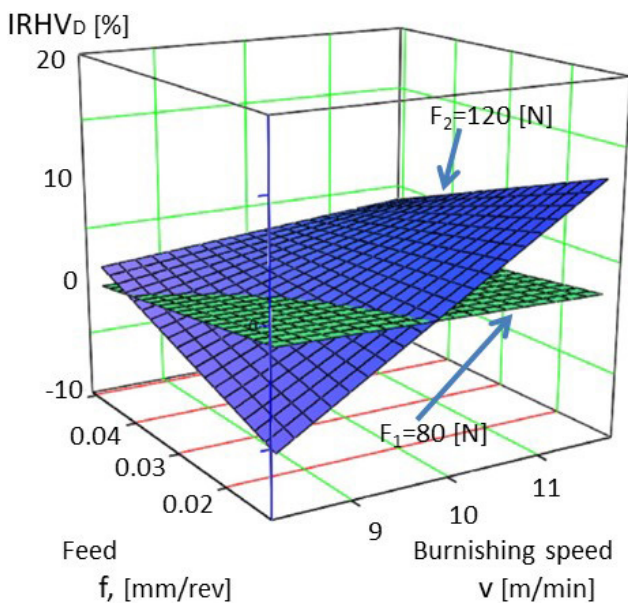


Fig. 7 Surface hardness improvement ratio (IRHV) for sample set D, as function of burnishing speed (v), and feed (f), according to experimental formula Eq. (6)

Electron microscopic images were taken to observe morphological changes, because structure of the surface influences hardness, and additionally it affects deviation of hardness measurements. Bottom part of Fig. 9 demonstrates original surface of side of sample cylinders. Partly melted and adhered metal particles and quite uneven surface can be observed.

Fig. 10 and Fig. 11 show electron microscopic images of polished cross sections.

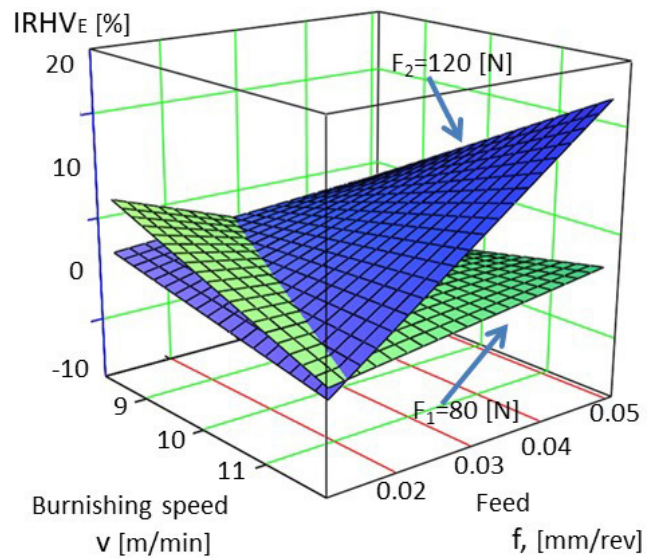


Fig. 8 Surface hardness improvement ratio (IRHV) for sample set E, as function of burnishing speed (v), and feed (f), according to experimental formula Eq. (7)

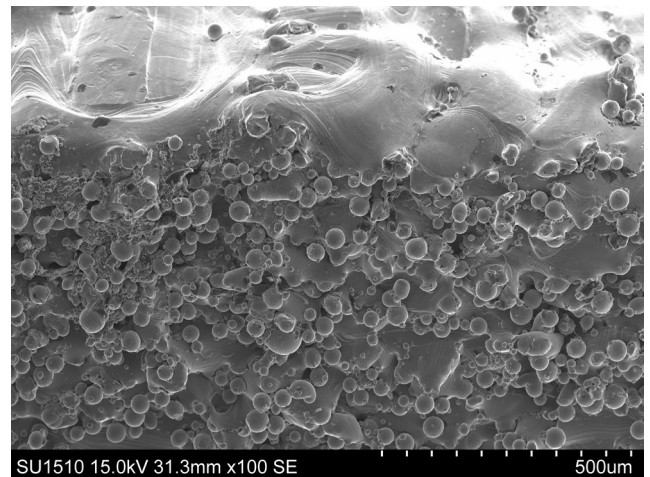


Fig. 9 Electron microscopic image of the original surface of a sample: On the upper part the top of the cylinder can be seen, what lays in the plane of layers melted during the production procedure. Bottom part of the picture shows the side of the cylinder, which is perpendicular to layers of manufacturing. This surface was postprocessed by burnishing

Four main types of morphological changes can be observed:

1. Burnishing cause plastic deformation of a top (protrusion) on original surface, bends it down, and sometimes remained powder particles are deformed (notation on figures: T).
2. Valleys originally existing on the surface may be decreased (attenuated) by removing partly upper brim of those (notation on figures: V).
3. Holes (cavities) can be formed by deformation, that is bending down of protrusions. Originally open valleys may be closed and form an inner hole (notation on figures: H).

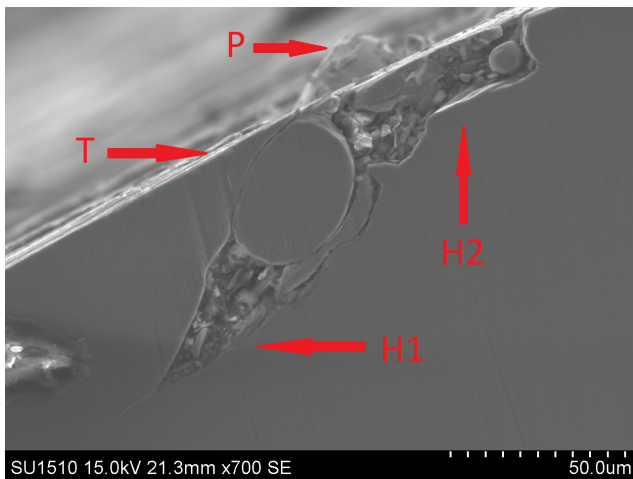


Fig. 10 Electron microscopic image on a cross section of sample E1: Label T points to a plastically deformed part, which was antecedently a protrusion, H1 indicates an inner hole enclosed by deformation of the proper protrusion (T), H2 shows a hole, which was partly open (even before polishing), P shows a protrusion. Possibly before burnishing H1 and H2 belonged to a single hole, and plastic imprinting of T separated it into two parts.

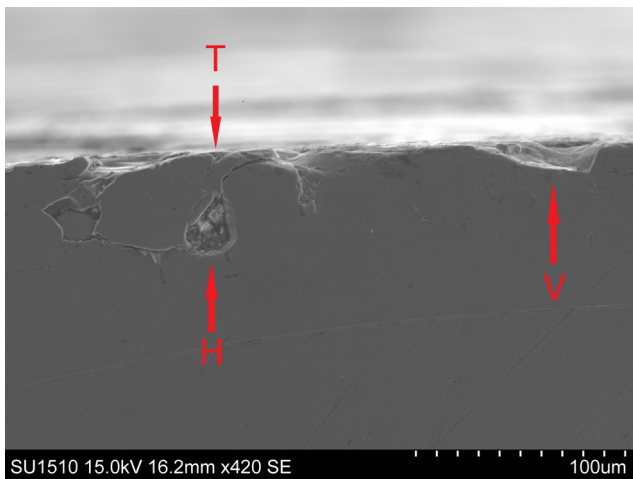


Fig. 11 Electron microscopic image taken on a cross section of sample A1: Label T points to a plastically deformed part, which was antecedently a top, H indicates an inner hole, V denotes a surface valley which was attenuated by burnishing.

4. Protrusions may be observed on the surface for two reasons. First, original ones may partly remain. Second, relatively small protrusions may be created by the ploughing-like movement of the diamond tool (notation on figures: P).

Changes in the structure of the surface may make effect to surface hardness in multiple way:

1. First, pushing down protrusions makes the surface more compact, may eliminate holes or valleys so increasing hardness.

2. Second, attenuating or possibly totally removing valleys improves surface hardness.
3. Third, formation of inner holes by plastic deformation of protrusions generates non-visible vacancies just under the surface, which cause instability of solidity. These vacancies may collapse under load, which implies decrease in hardness, and also influences measurements.
4. Remaining or generated protrusions influence hardness indirectly by making the surface uneven.

A comparison of the specimen produced in 5 different additive manufacturing parameter combinations was performed by comparing the maximum hardness improvements achieved with 8 different burnishing technology parameter combinations. According to this, we were able to see the greatest value of the maximum improvement (IRHV = 18.73%) in the hardness of diamond burnished on the specimens produced with the additive technology B – infill laser power was medium (280 W), infill laser speed the smallest (1000 mm/s) and energy input the largest (66.667 W/mm³). Where the burnishing technology parameters were as follows: $v = 11,775$ m/min; feed $f = 0.0125$ mm/rev and burnishing force $F = 120$ N.

In this respect, the smallest maximum hardness improvement (IRHV = 7.21%) of diamond burnishing was obtained on the test specimens produced with the additive technology D. The additive technological parameters in case of specimen D are: infill laser power was medium (233.33 W), infill laser speed is the lowest (1000 mm/s) and energy input is 55.556 W/mm³.

6 Summary and conclusions

The surface hardness of parts made by additive manufacturing was examined before and after surface modification executed by diamond burnishing. The cylindrical shape specimens were made by selective laser melting from Ti6Al4V. The specimens were manufactured with five (signed A, B, C, D and E) different SLM manufacturing parameters and 8 specimens were prepared and tested in each case. Sliding friction burnishing was chosen for the post-machining of the surfaces of specimens A–E. The parameters of diamond burnishing were determined by a three-factor, two-level full factorial experimental design. During diamond burnishing the burnishing speed, feed, and burnishing force were varied. This means that for each combination of different SLM manufacturing parameters, a diamond burnishing operation with 8 different parameters was performed. The surface

Vickers hardness of HV10 was measured before and after burnishing on a hardness measuring equipment type HPO-250. Based on the HV10 surface hardness values, the surface hardness improvement ratios were calculated for each case.

It can be stated that from additive technological point of view the largest energy input (66.667 W/mm^3) was the most advantageous. From burnishing technological point of view the larger burnishing force ($F = 120 \text{ N}$), the largest burnishing speed $v = 11,775 \text{ m/min}$ and the smaller feed $f = 0.0125 \text{ mm/rev}$ serve the best result.

By diagrams Figs. 4–8, it is ascertainable that how burnishing parameters influence surface hardness improvement in case of each SLM production parameter set (A–E sample sets). We can formulate the following statements:

1. Maximum surface hardness improvement can be reached by applying $F = 120 \text{ N}$ burnishing force in each production cases (A–E) investigated in this study.
2. Other burnishing parameters influence surface hardness change in different ways:
 - In case of sample set A, smaller v (burnishing speed) and f (feed) is necessary for achieving surface hardness improvement.
 - In case of sample set B, larger v and smaller f is necessary for maximum surface hardness improvement.
 - In case of sample sets C and D, it is advisable for small v large f , and for large v small f .
 - In case of sample set E, increase of both v and f is necessary in order to achieve maximum surface hardness improvement.

References

- [1] Vafadar, A., Guzzomi, F., Rassau, A., Hayward, K. "Advances in Metal Additive Manufacturing: A Review of Common Processes, Industrial Applications, and Current Challenges", Applied Sciences, 11(3), 1213, 2021.
<https://doi.org/10.3390/app11031213>
- [2] Yap, C. Y., Chua, C. K., Dong, Z. L., Liu, Z. H., Zhang, D. Q., Loh, L. E., Sing, S. L. "Review of selective laser melting: Materials and applications", Applied Physics Reviews, 2(4), 041101, 2015.
<https://doi.org/10.1063/1.4935926>
- [3] Buican, G. R., Oancea, G., Lancea, C., Pop, M. A. "Influence of Layer Thickness on Internal Structure of Parts Manufactured from 316-L Steel Using SLM Technology", Applied Mechanics and Materials, 809–810, pp. 369–374, 2015.
<https://doi.org/10.4028/www.scientific.net/AMM.809-810.369>
- [4] Singla, A. K., Banerjee, M., Sharma, A., Singh, J., Bansal, A., Gupta, M. K., Khanna, N., Shahi, A. S., Goyal, D. K. "Selective laser melting of Ti6Al4V alloy: Process parameters, defects and post-treatments", Journal of Manufacturing Processes, 64, pp. 161–187, 2021.
<https://doi.org/10.1016/j.jmapro.2021.01.009>
- [5] Beaucamp, A. T., Namba, Y., Charlton, P., Jain, S., Graziano, A. A. "Finishing of additively manufactured titanium alloy by shape adaptive grinding (SAG)", Surface Topography: Metrology and Properties, 3(2), 024001, 2015.
<https://doi.org/10.1088/2051-672X/3/2/024001>
- [6] Qu, N. S., Fang, X. L., Zhang, Y. D., Zhu, D. "Enhancement of surface roughness in electrochemical machining of Ti6Al4V by pulsating electrolyte", The International Journal of Advanced Manufacturing Technology, 69(9–12), pp. 2703–2709, 2013.
<https://doi.org/10.1007/s00170-013-5238-9>
- [7] Pyka, G., Kerckhofs, G., Papanтониou, I., Speirs, M., Schrooten, J., Wevers, M. "Surface Roughness and Morphology Customization of Additive Manufactured Open Porous Ti6Al4V Structures", Materials, 6(10), pp. 4737–4757 2013.
<https://doi.org/10.3390/ma6104737>
- [8] Varga, G., Dezső, G., Szigeti, F. "Surface Roughness Improvement by Sliding Friction Burnishing of Parts Produced by Selective Laser Melting of Ti6Al4V Titanium Alloy", Machines, 10(5), 400, 2022.
<https://doi.org/10.3390/machines10050400>

- [9] Cosma, C., Balci, N., Moldovan, M., Morovic, L., Gogola, P., Miron-Borzan, C. "Post-processing of customized implants made by laser beam melting from pure Titanium", *Journal of Optoelectronics and Advanced Materials*, 19(11–12), pp. 738–747, 2017. [online] Available at: <https://joam.inoe.ro/articles/post-processing-of-customized-implants-made-by-laser-beam-melting-from-pure-titanium/> [Accessed: 15 August 2022]
- [10] Zhang, H., Dong, D., Su, S., Chen, A. "Experimental study of effect of post processing on fracture toughness and fatigue crack growth performance of selective laser melting Ti-6Al-4V", *Chinese Journal of Aeronautics*, 32(10), pp. 2383–2393, 2019. <https://doi.org/10.1016/j.cja.2018.12.007>
- [11] Jagadeesh, G. V., Gangi Setti, S. "A review on latest trends in ball and roller burnishing processes for enhancing surface finish", *Advances in Materials and Processing Technologies*, 2022. <https://doi.org/10.1080/2374068X.2022.2077534>
- [12] Maximov, J. T., Duncheva, G. V., Anchev, A. P., Ganev, N., Amudjev, I. M., Dunchev, V. P. "Effect of slide burnishing method on the surface integrity of AISI 316Ti chromium–nickel steel", *Journal of the Brazilian Society of Mechanical Science and Engineering*, 40(4), 194, 2018. <https://doi.org/10.1007/s40430-018-1135-3>
- [13] Dzierwa A., Markopoulos, A. P. "Influence of Ball-Burnishing Process on Surface Topography Parameters and Tribological Properties of Hardened Steel", *Machines*, 7(1), 11, 2019. <https://doi.org/10.3390/machines7010011>
- [14] Kato, H., Hirokawa, W., Todaka, Y., and Yasunaga, K. "Improvement in Surface Roughness and Hardness for Carbon Steel by Slide Burnishing Process", *Materials Sciences and Applications*, 12(5), pp. 171–181, 2021. <https://doi.org/10.4236/msa.2021.125011>
- [15] Zaleski, K., Skoczylas, A. "Effect of Slide Burnishing on the Surface Layer and Fatigue Life of Titanium Alloy Parts", *Advances in Materials Science*, 19(4), pp. 35–45, 2019. <https://doi.org/10.2478/adms-2019-0020>
- [16] Revankar, G. D., Shetty, R., Rao, S. S., Gaitonde, V. N. "Wear resistance enhancement of titanium alloy (Ti–6Al–4V) by ball burnishing process", *Journal of Materials Research and Technology*, 6(1), pp. 13–32, 2017. <https://doi.org/10.1016/j.jmrt.2016.03.007>
- [17] Rotella, G., Caruso, S., Del Prete, A., Filice, L. "Prediction of Surface Integrity Parameters in Roller Burnishing of Ti6Al4V", *Metals*, 10(12), 1671, 2020. <https://doi.org/10.3390/met10121671>
- [18] Sanguedolce, M., Rotella, G., Saffioti, M. R., Filice, L. "Functionalized additively manufactured parts for the manufacturing of the future", *Procedia Computer Science*, 180, pp. 358–365, 2021. <https://doi.org/10.1016/j.procs.2021.01.174>
- [19] Sanguedolce, M., Rotella, G., Saffioti, M. R., Filice, L. "Burnishing of AM materials to obtain high performance part surfaces", *Journal of Industrial Engineering and Management*, 15(1), pp. 73–89, 2022. <https://doi.org/10.3926/jiem.3608>
- [20] Rotella, G., Filice, L., Micari, F. "Improving surface integrity of additively manufactured GP1 stainless steel by roller burnishing", *CIRP Annals*, 69(1), pp. 513–516, 2020. <https://doi.org/10.1016/j.cirp.2020.04.015>
- [21] Saffioti, M. R., Sanguedolce, M., Rotella, G., Filice, L. "On the Effects of Burnishing Process on Tribological Surface Resistance of Additively Manufactured Steel", presented at ESAFORM 2021. 24th International Conference on Material Forming, Liège, Belgium, Apr., 14–16, 2021. [online] Available at: <https://popups.uliege.be/esaform21/index.php?id=1903> [Accessed 25 August 2022]
- [22] Teramachi, A., Yan, J. "Improving the Surface Integrity of Additive-Manufactured Metal Parts by Ultrasonic Vibration-Assisted Burnishing", *Journal of Micro and Nano-Manufacturing*, 7(2), 024501, 2019. <https://doi.org/10.1115/1.4043344>
- [23] Karthick Raaj, R., Vijay Anirudh, P., Karunakaran, C., Kannan, C., Jahagirdar, A., Joshi, S., Balan, A. S. S. "Exploring grinding and burnishing as surface post-treatment options for electron beam additive manufactured Alloy 718", *Surface and Coatings Technology*, 397, 126063, 2020. <https://doi.org/10.1016/j.surfcoat.2020.126063>
- [24] Liu, S., Shin, Y. C. "Additive manufacturing of Ti6Al4V alloy: A review", *Materials & Design*, 164, 107552, 2019. <https://doi.org/10.1016/j.matdes.2018.107552>
- [25] Bruschi, S., Bertolini, R., Bordin, A., Medea, F., Ghiotti, A. "Influence of the machining parameters and cooling strategies on the wear behavior of wrought and additive manufactured Ti6Al4V for biomedical applications", *Tribology International*, 102, pp. 133–142, 2016. <https://doi.org/10.1016/j.triboint.2016.05.036>
- [26] Shunmugavel, M., Polishetty, A., Nomani, J., Goldberg, M., Littlefair, G. "Metallurgical and Machinability Characteristics of Wrought and Selective Laser Melted Ti-6Al-4V", *Journal of Metallurgy*, 2016, 7407918, 2016. <https://doi.org/10.1155/2016/7407918>
- [27] Kandeve, M., Kostadinov, G., Penyashki, T., Kamburov, V., Dimitrova, R., Valcanov, S., Nikolov, A., Elenov, B., Petrzhih, M. "Abrasive Wear Resistance of Electrospark Coatings on Titanium Alloys", *Tribology in Industry*, 44(1), pp. 132–142, 2022. <https://doi.org/10.24874/ti.1143.06.21.09>
- [28] Hebei Metals Industrial Limited "Titanium Alloy: Ti-6Al-4V", [online] Available at: <http://www.metalspiping.com/titanium-alloy-ti-6al-4v.html> [Accessed: 15 August 2022]
- [29] Maximov, J. T., Anchev, A. P., Duncheva, G. V., Ganev, N., Selimov, K. F. "Influence of the process parameters on the surface roughness, micro-hardness, and residual stresses in slide burnishing of high-strength aluminum alloys", *Journal of the Brazilian Society of Mechanical Sciences and Engineering*, 39(8), pp. 3067–3078, 2017. <https://doi.org/10.1007/s40430-016-0647-y>
- [30] Rotella, G., Rinaldi, S., Filice, L. "Roller burnishing of Ti6Al4V under different cooling/lubrication conditions and tool design: effects on surface integrity", *The International Journal of Advanced Manufacturing Technology*, 106(1–2), pp. 431–440, 2020. <https://doi.org/10.1007/s00170-019-04631-z>

- [31] Samatham, M., Ashok Kumar, U., Pappula, L. "Critical review on different burnishing processes of Ti-6Al-4V Alloy", *International Journal of Scientific Research in Science, Engineering and Technology*, 7(1), pp. 266–273, 2020.
<https://doi.org/10.32628/IJSRSET20721>
- [32] Toboła, D., Morgiel, J., Maj, L. "TEM analysis of surface layer of Ti-6Al-4V ELI alloy after slide burnishing and low-temperature gas nitriding", *Applied Surface Science*, 515, 145942, 2020.
<https://doi.org/10.1016/j.apsusc.2020.145942>
- [33] Hungarian Standards Institute (MSZT) "MSZ EN ISO 6507-1: 2018 Fémek. Vickers-keménységmérés. 1. rész: Mérési eljárás" (MSZ EN ISO 6507-1:2018 Metallic materials. Vickers hardness test. Part 1: Test method), MSZT, Budapest, Hungary, 2018.
- [34] Dezső, G., Szigeti, F., Varga, G. "Measurement of the surface hardness of titanium alloy samples produced by additive manufacturing", [pdf] In: Gáti, J. (ed.) XXXI. Nemzetközi Hegesztési Konferencia, Kecskemét, Hungary, 2022, pp. 17–24. ISBN 978-615-6260-01-7 Available at: https://maheg.hu/wp-content/uploads/2022/10/XXXI_Hegkonf_kiadvany.pdf [Accessed: 15 August 2022]